

Surface-Resonance Fine Structure in Low-Energy Electron Diffraction*

J. Rundgren and G. Malmström

Department of Theoretical Physics, Royal Institute of Technology, S-100 44 Stockholm 70, Sweden

(Received 26 October 1976)

We demonstrate that the reflection of electrons from the image potential barrier outside the surface of a metal crystal induces a surface-resonance fine structure in the low-energy electron diffraction intensity profiles just below the energy of emergence of a new beam. The resonance levels are arranged in a Rydberg series with the constant $\frac{1}{16}$ Ry. The beam emergence from aluminum (001) near 18 eV is calculated and comparison with measured resonances is sought.

A number of experiments on the reflection of low-energy electrons from metal surfaces¹⁻⁴ have demonstrated that the emergence of a nonspecular beam in a low-energy electron diffraction (LEED) pattern is often, if not always, accompanied by the occurrence of a fine structure in the intensity of the specular beam that extends over 1-2 eV or more below the energy of emergence. McRae⁵ explained this fine structure as a surface-resonance phenomenon, namely, as an effect of multiple scattering in a wave guide bounded on one side by the potential barrier towards the vacuum and on the other side by the outermost atomic layer which can be considered to represent the reflectivity of the bulk. McRae first approximated the vacuum side of the wave guide by a real exponential potential; Jennings⁶ and Jennings and Read⁶ later utilized the image potential, and recently McRae and Caldwell⁷ considered the image potential together with an imaginary electron self-energy of a Gaussian termination in the vacuum. Below and above the surface plasmon threshold the reflectivity of the bulk can exhibit structures having energy widths of the order of 1 and 10 eV,⁵ respectively. In this manner fine structures have been interpreted as surface resonances at very low energies³; but there are also experiments^{2,4} showing fine structures as narrow as 1-2 eV above the plasmon threshold.

Our calculations of the transmission and reflection by the surface barrier of a metal are based on a one-electron optical potential of the following form. The crystal may occupy the half-space $z > 0$ extending inwards from half an interlayer spacing outside the topmost atomic layer, and we suppose that geometrically the surface barrier potential can be considered as a function of z only. The real part of the potential is assumed to terminate in the image potential $\frac{1}{4}e^2z^{-1}$ ($z < 0$) towards the vacuum and to join smoothly to a constant interlayer potential V_0 in the manner

established by Lang and Kohn.⁸ The imaginary part of the surface barrier potential has a different asymptotic behavior in the vacuum depending on whether the electrons propagate at near normal or near glancing incidence, namely, proportional to $-z^{-2}$ or to $-|z|^{-1/2} \exp(z/c)$ ($c > 0$), as shown, respectively, by Inkson⁹ and by Echenique and Pendry.¹⁰ Around $z = 0$ there is a smooth transition into a constant imaginary value $i\beta_0$. In the LEED calculations illustrating beam emergences we utilize an exponential absorptive tail for all beams; the results prove very similar if a z^{-2} tail is used.

A very important feature of the surface barrier is its reflectivity r^{+-} which gives the backscattered companion $r^{+-} \exp[i\vec{k} \cdot (x, y, -z)]$ of a beam $\exp[i\vec{k} \cdot (x, y, z)]$ propagating from within the crystal towards the vacuum. r^{+-} is a function of $E_{\perp} = E - \frac{1}{2}|\vec{k}_{\parallel}|^2$, where E is the primary energy and \vec{k}_{\parallel} , parallel to the $O-x-y$ plane, designates the surface component of the wave vector \vec{k} of the beam under consideration. The electron waves in the vacuum far away from the surface are represented by Whittaker functions.¹¹ From their asymptotic behavior for small real and imaginary $k_{\perp} = E_{\perp}^{1/2}$ we deduce that $r^{+-}(E_{\perp})$ tends to a fixed complex value when $E_{\perp} \rightarrow 0$ from the positive side, whereas $r^{+-}(E_{\perp})$ approaches a limiting circle in the complex plane when $E_{\perp} \rightarrow 0$ from the negative side. It turns out that $r^{+-}(E_{\perp})$ makes one revolution on its limiting circle for each energy level $E_{\perp} = E_n$ of the Rydberg series

$$E_n = -\frac{1}{16}(a+n)^{-2} \text{ Ry}, \quad (1)$$

where $n = 1, 2, \dots$ and, to a good approximation, $0 < a < 1$. Although the surface barrier is absorptive, the levels E_n become sharply defined, because the reflections from the image potential take place outside the range of both the exponential and the z^{-2} tail. The radius of the limiting circle of r^{+-} depends on the strength and, to a

lesser degree, on the shape of the absorptive tail. Generally the center of the limiting circle is somewhat displaced from the origin $r^{+-} = 0$.

For the surface barrier of aluminum and primary energies near 18 eV we have chosen the inner potential $-12 - i4$ eV and an exponential absorptive tail of range $c = 0.63$ Å. A smooth model is used for the potential across the surface. We find that in this case r^{+-} has the limiting circle $|r^{+-} - (0.00, 0.06)| = 0.45$ below $E_{\perp} = 0$ and the limit $(-0.09, 0.02)$ above $E_{\perp} = 0$.

As shown by McRae⁵ the reflection from a crystal in the presence of a surface barrier is determined essentially by the multiple scattering matrix $X = (1 - r^{+-}R^{-+})^{-1}$, where r^{+-} and R^{-+} are matrices in the beam representation accounting for the crystal-to-crystal reflectivity of the surface barrier and of the vacuum-to-vacuum reflectivity of the crystal bulk. Since the surface barrier is supposed to be a plane, the matrix r^{+-} is diagonal and has elements $r_{\vec{g}}^{+-}$ corresponding to the energies $E_{\perp\vec{g}} = E - \frac{1}{2}|\vec{k}_{\parallel} + \vec{g}|^2$ of the beams \vec{g} . Our calculations show that $|r_{\vec{g}}^{+-}|$ is large on the limiting circle corresponding to the energies -1 eV $< E_{\perp\vec{g}} < 0$ eV as well as on a piece of curve in the adjacent energy range -8 eV $< E_{\perp\vec{g}} < -1$ eV. Under these circumstances we can imagine three cases where the elements of X exhibit rapid variations with energy. (i) E greater than the plasmon threshold: $1 - r^{+-}R^{-+}$ having eigenvalues not near to zero and a $r_{\vec{g}}^{+-}$ revolving on the limiting circle. A modulation of X corresponding to the levels of the Rydberg series (1) then will result. This type of fine structure is analogous to the Rydberg series of electronic surface states outside the surface of an insulator as was recently experimentally established for liquid helium.¹² (ii) E less than the plasmon threshold: $1 - r^{+-}R^{-+}$ having an eigenvalue near to zero and no $r_{\vec{g}}^{+-}$ situated on the limiting circle but some $r_{\vec{g}}^{+-}$ moving on its -8 to -1 eV tail. In this case a single surface resonance of the Breit-Wigner type would occur as pointed out by McRae.⁵ (iii) In addition, a hybrid between the previous two cases conceivably would occur when the condition E less than the plasmon threshold gives a high reflectivity R^{-+} and simultaneously $r_{\vec{g}}^{+-}$ revolves on the limiting circle.

Using matrix algebra we deduce that the elements of X , and hence also the amplitudes of the LEED beams, all tend to limiting circles like $r_{\vec{g}}^{+-}$ when $E_{\perp\vec{g}}$ takes values within the range of the Rydberg series (1). In case (i), where the elements of R^{-+} have structures whose widths

are of the order of 10 eV, the amplitudes will spiral in very quickly towards the limiting circles. Our LEED calculations¹³ indeed bear out this picture, and the calculated LEED intensity profiles exhibit a distribution of intensity fringes corresponding to the Rydberg series (1) below the energy of emergence $E_{\perp\vec{g}} = 0$. The distribution depends on the reflectivity R^{-+} of the bulk and will hence look different for different materials. Experimental observation of the fringes $n = 1, 2$ will require a resolving power of 0.1 eV.

Figure 1 illustrates surface-resonance fine structures calculated for the beam emergences from the (001) surface of aluminum near 18 eV. The intensities of all the visible beams are superposed as in a total yield experiment. Normal and tilted incidence (rotation about the [110] axis) are demonstrated. Figure 1 indicates that the surface-resonance fine structure is very sensitive to tilts which break the symmetry of the pattern of emerging beams. For example, on a 0.5-deg tilt the emergences of the two beams not on the [110] axis move ± 0.3 eV in energy. In the specular intensity profile, therefore, several fine structures distributed as E_n and mutually displaced by some tenths of an eV will add largely destructively. According to our calculations the emergence of a beam causes modulation of not only the specular beam but of all other beams

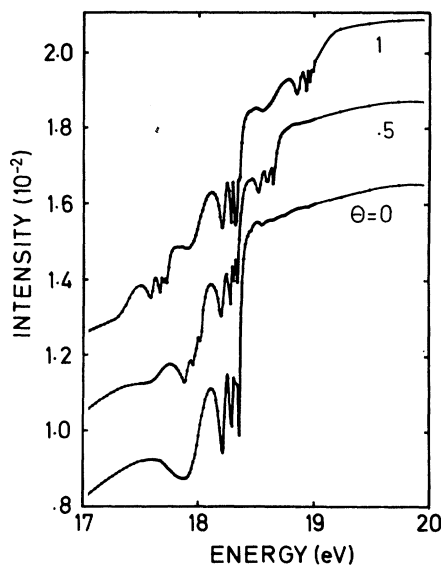


FIG. 1. Calculated intensity profiles of the specular and nonspecular beams from the (001) surface of aluminum are drawn superposed as in a total yield experiment. Tilts about the [110] axis by $\theta = 0, 0.5$, and 1 deg from the normal are illustrated.

that appeared at lower energies.

A method of measuring total yield (Henrich² and McRae and Caldwell³) utilizes differentiation of the total intensity I with respect to the primary energy E . We have simulated the procedure by applying smoothing and differentiation to $I(E)$ in Fig. 1, and we have obtained dI/dE curves having double peaks at 18 eV as was observed by Henrich in his experiment on aluminum. Our smoothing was done by means of convolution of $I(E)$ with a Gaussian of standard deviation $\sigma=0.25$ eV corresponding to the measured resonance width 0.5 eV. With this σ , however, $I(E)$ curves calculated on one hand with a surface barrier and on the other with the no-reflection boundary condition turned out to produce very similar dI/dE curves because of the stepwise rise of intensity at the emergence.

The structure of the total yield is better analyzed by means of high-pass filtration of $I(E)$ to remove the background of the beam thresholds as was demonstrated recently by McRae, Landwehr, and Caldwell in an experiment on oxygenated nickel (001).⁴ We have processed the $I(E)$ curves in Fig. 1 in an analogous manner by applying numerically a high-pass filter of a Gaussian characteristic ($\sigma=0.25$ eV). Figure 2 shows the result by means of two sets of curves representing instrumental resolving powers of $\sigma=0.01$ and

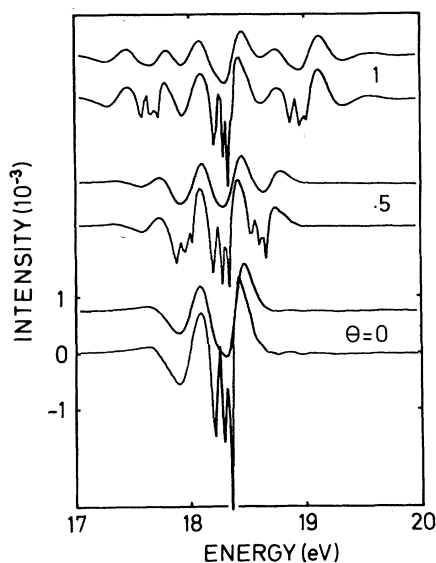


FIG. 2. The superposed beam intensities have been filtered by a high-pass filter removing background structures broader than 0.3 eV. Shown are filtered data simulating instrumental resolving powers of 0.02 and 0.1 eV.

0.05 eV. In the latter case where just the levels $n=1, 2$ of the Rydberg spectrum are resolved, we note a resemblance to the curves obtained by McRae, Landwehr, and Caldwell. This we expect since the Rydberg spectrum (1) applies to all metal surfaces. The filter characteristics are found⁴ not to be a critical feature of this method of disentangling the fine structure from the background.

In summary, our calculation of a Rydberg spectrum of surface resonances in LEED is based on the following concepts: outside a metal surface an optical potential barrier terminating in the image potential; a wave guide limited by the surface barrier and the crystal bulk; the layer-by-layer method for calculating LEED. In this picture our deduction that the crystal-to-crystal reflectivity of the surface barrier and the reflected beam amplitudes revolve on limiting circles, when E increases to an energy of emergence, represents an exact solution of the one-electron Schrödinger equation. We therefore believe that a Rydberg spectrum of surface resonances will accompany every emergence of a new beam from the plane surface of a metal crystal. The constant of the spectrum is $\frac{1}{16}$ Ry. Our suggestion is supported by the result of a recent total yield experiment on oxygenated nickel (001).⁴

*Work supported by the Swedish National Science Research Council.

¹E. G. McRae and C. W. Caldwell, *Surf. Sci.* **7**, 41 (1967); S. Andersson, *Surf. Sci.* **19**, 21 (1970); J. Lauzier, L. de Bersuder, and V. Hoffstein, *Phys. Rev. Lett.* **27**, 735 (1971); E. G. McRae and G. H. Wheatley, *Surf. Sci.* **29**, 342 (1972); S. Sinharoy, R. M. Stern, and P. D. Goldstone, *Surf. Sci.* **30**, 207 (1972).

²V. E. Henrich, *Surf. Sci.* **49**, 675 (1975).

³E. G. McRae and C. W. Caldwell, *Surf. Sci.* **57**, 63 (1976).

⁴E. G. McRae, J. M. Landwehr, and C. W. Caldwell, to be published.

⁵E. G. McRae, *Surf. Sci.* **25**, 491 (1971).

⁶P. J. Jennings, *Surf. Sci.* **25**, 513 (1971); P. J. Jennings and M. N. Read, *Surf. Sci.* **41**, 113 (1974).

⁷E. G. McRae and C. W. Caldwell, *Surf. Sci.* **57**, 77 (1976).

⁸N. D. Lang and W. Kohn, *Phys. Rev. B* **1**, 4555 (1970).

⁹J. C. Inkson, *J. Phys. F* **3**, 2143 (1973).

¹⁰P. M. Echenique and J. B. Pendry, *J. Phys. C* **8**, 2936 (1975).

¹¹L. J. Slater, *Confluent Hypergeometric Functions*

(Cambridge Univ. Press, Cambridge, England, 1960).
¹²C. C. Grimes, T. R. Brown, M. L. Burns, and C. L. Zipfel, Phys. Rev. B **13**, 140 (1976).

¹³The computer program is described by J. Rundgren and A. Salwén, Comput. Phys. Commun. **9**, 312 (1974), and J. Phys. C **9**, 3701 (1976).

Anisotropy of Surface Self-Diffusion on Ni(110)

E. E. Latta and H. P. Bonzel

Institut für Grenzflächenforschung und Vakuumphysik, Kernforschungsanlage Jülich, 517 Jülich, Germany

(Received 28 December 1976)

The theoretically expected directional anisotropy of surface self-diffusion was experimentally verified for a clean Ni(110) surface. The diffusion coefficients were determined by the sinusoidal profile decay technique at 800°C in [001] and [1 $\bar{1}$ 0] directions as 2.2×10^{-7} cm² sec⁻¹ and 3.0×10^{-6} cm² sec⁻¹, respectively. The cleanliness and structural integrity of the Ni(110) surface were checked with Auger spectroscopy and low-energy electron diffraction, respectively.

The best demonstration of the directional anisotropy of surface self-diffusion of metals has emerged from field-ion microscopy measurements.^{1,2} In these experiments no significant migration of adatoms across close-packed rows, e.g., on the (211) surface of tungsten¹ or the (110) surface of rhodium,² has been reported. Adatom migration occurs exclusively parallel to close-packed rows. Thus there is strong but qualitative evidence for the directional anisotropy of surface self-diffusion. By comparison, there have also been a number of mass-transfer diffusion studies devoted to this subject,³⁻⁶ but large directional anisotropy effects have never been found with these techniques.

In this Letter we report the first quantitative demonstration of the directional anisotropy of surface self-diffusion by the example of a clean Ni(110) surface. The mass-transfer diffusivities obtained by the *in situ* sinusoidal profile technique⁷ at 800°C are about a factor of 14 larger in the [1 $\bar{1}$ 0] direction than in the [001] direction; this factor increases with decreasing temperature. This result is in contrast to a previous investigation of the directional anisotropy of surface self-diffusion on Ni(110) by the same technique.⁶ It is believed that the major reason for being able now to establish this directional anisotropy effect on Ni(110) is the improved surface cleanliness during the diffusion runs and the lower temperature of measurement.

The surface self-diffusion coefficients, D_s , were measured by the sinusoidal profile technique.⁸ This technique is well suited for the study of directional anisotropy since it permits establishment of one-dimensional chemical po-

tential gradients on the surface. A number of profiles with periodicities of 4.0, 5.4, 7.0, and 9.0 μm were etched into the smooth surface of a Ni(110) crystal which was oriented to within 0.3° and polished to a mirrorlike finish. The procedure for making such profiles has been described in detail elsewhere.⁹ The uniformity of profile amplitudes (in a range of 0.3–0.6 μm) was checked by interference microscopy. The grooves of the profile were oriented parallel to either the [1 $\bar{1}$ 0] or [001] direction. The so-prepared Ni(110) crystals were mounted in an ultra-high vacuum system of base pressure 1×10^{-8} Pa. During a diffusion run the amplitude of the profile was determined *in situ* at temperature via the intensity distribution of a laser diffraction pattern.⁷ The temperature was measured with a Pt vs Pt-10% Rh thermocouple spotwelded to the crystal.

Prior to each diffusion experiment the crystal surface was cleaned by argon-ion bombardment and brief heating cycles to about 700–900°C depending on which diffusion direction was going to be studied. Sulfur and phosphorus were detected initially by Auger spectroscopy (AES) as major impurities. During a diffusion run the surface cleanliness was checked periodically and a sputter cycle was chosen when necessary. In general the maximum coverage of sulfur during the diffusion experiment was estimated to remain below 15%. Sulfur had no influence on the diffusion rate since no change in the rate was observed before and after sputter cleaning of the surface.

The surface structure of the Ni(110) crystals as well as the directional orientation of the sinusoidal profiles was verified with low-energy